

Chapter 8

History of the South China Sea – A Synthesis

Pinxian Wang and Qianyu Li

Introduction

An overwhelming part of our current knowledge on the geoclimatic history of the South China Sea (SCS) was generated over the last 20–30 years. The amount of paleoceanographic and paleoclimatic data available is tremendous and is still emerging rapidly. A comprehensive synthesis of these data is not easy because the proxy records need to be properly interpreted first. For example, to differentiate whether the observed changes in the SCS were caused by global, regional or local factors remains as a challenge.

For a long time, the prevalent history of the SCS basin has been reconstructed mainly based on geophysical data, and the history of the East Asian monsoon on terrestrial records, in particular from the Chinese Loess Plateau. Now, deep-sea sediment sequences recovered during ODP Leg 184 not only provide the first direct record of the formation and evolution of the SCS deep water basin but also the first long marine record of the East Asian monsoon history (Wang P. et al. 2003). The present chapter attempts to present an integrated history of the SCS basin and the East Asian Monsoon by synthesizing all available data presented in previous chapters of this volume. The perspective and importance of the SCS for recognition of continent-ocean interactions in the Asia–West Pacific in a historical aspect are also briefly discussed.

P. Wang (✉)

State Key Laboratory of Marine Geology, Tongji University, Shanghai 200092, China
e-mail: pxwang@online.sh.cn; pxwang@tongji.edu.cn

Q. Li

State Key Laboratory of Marine Geology, Tongji University, Shanghai 200092, China;
School of Earth and Environmental Sciences, The University of Adelaide,
South Australia 5005, Australia
e-mail: qli01@tongji.edu.cn; qianyu.li@adelaide.edu.au

8.1 Evolution of the South China Sea Basin

Broadly, the history of the SCS basin can be divided into three major stages: (1) a pre-spreading or rifting stage in the early Paleogene, (2) a seafloor spreading stage in the late Paleogene-early Miocene, and (3) a post-spreading or closing stage since the late Miocene (Chapter 2) (Table 8.1).

Table 8.1 Major stages of the SCS basin evolution are characterized by variations in basin morphology and sedimentation rates

Stage		Time (Ma)	Basin features	Sedimentation
Pre-spreading	Rifting	> 37	Rift basins only	Rapid
Spreading	Early spreading	37–28.5	A narrow deep water gulf	Rapid
	Ridge jump	28.5–23	Deepening and deformation	Slumping and hiatuses
	Late spreading	23–16	Increase in size, terminated by collision in the south	Slow; coral reef development
Post-spreading	Closing	16–6.5	Deformation in the south	Slow
		< 6.5	Closure on the eastern side	Slow
		< 3	Development of deltas and broad shelves	Increased terrigenous input

Pre-Spreading Stage in the Early Paleogene

The history of the SCS started from rifting in the Paleocene with the formation of a number of parallel rift basins along the South China continental margin. Filled with thick non-marine deposits of mainly Paleogene age, these rift basins now become the main hydrocarbon producers in the northern and western SCS. While most of the rift basins failed after the Paleogene, one or several of them in the northeast developed further into the modern South China Sea basin as a result of seafloor spreading. Earlier studies of magnetic anomalies in the SCS central basin indicated that seafloor spreading began at ~30 Ma, anomaly C11 (Chapter 2). However, the unexpected discovery of bathyal fauna in the lowermost core at ODP Site 1148, at the foot of the northern SCS slope, implies the onset of the SCS breakup at least 33 Ma ago, in the earliest Oligocene (Li Q. et al. 2006). The probable existence of oceanic crust in the northeastern corner with magnetic anomaly C17 (Fig. 2.25) suggests an inception of seafloor spreading as early as 37 Ma, in the late Eocene (Hsu et al. 2004). If confirmed, the history of the SCS should be extended back beyond the Oligocene to nearly the middle/late Eocene boundary. Probably, the earliest marine basin in the present northeast during the late Eocene indeed co-existed to the south with the Proto-South China Sea, a broad shallow sea basin between the Nansha terrain (Dangerous Grounds) and islands of Borneo and Palawan and further south (Fig. 2.21). As recorded in ODP 1148 cores, the late Paleogene marine basin in the place of the present northern SCS was a narrow gulf with rapid accumulation of

bathyal deposits. Occasional transgressions during this stage might have left marine sediments with a broader spatial coverage, which explains the finding of an Eocene nannofossil zone in Well HJ15-11 from a neighboring rift center (Huang L. 1997).

Seafloor Spreading in the Oligocene-Early Miocene

Up to now, there is no unanimously accepted age model and mechanism for the opening of the SCS basin. Hypotheses range from crustal thermal variations to slab pull of Asia-Pacific plate collision to pulling effects of Indochina's southeast extrusion (Chapter 2). The difficulty lies partly in the absence of intense tectonic activities associated with the inception of the seafloor spreading likely due to the inheritance of the existing deep-water rift basins by the newly opening basin.

The early spreading stage in the early Oligocene was characterized by high sedimentation rates of > 60 m/myr (Chapter 3). This period lasted for about 5 myr or longer and terminated with an unconformity at ~ 25 Ma in the late Oligocene. All this was followed immediately by a very active tectonic regime at 25–23 Ma (anomaly C7 and younger), probably relating to the southeast extrusion of Indochina and a major ridge jump to the southwest (Chapter 2).

The late Oligocene experienced the strongest tectonic deformation in the entire process of the basin formation of the SCS. Along with widespread slumps, several unconformities have together erased a record of about 3 myr at ODP Site 1148. Geochemical analyses indicate a drastic shift of sedimentary source provenances from the southwest (Indochina-Sundaland) and possibly also the southeast to the north (i.e., mainland China) (Li X. et al. 2003). A similar sediment provenance change is also recorded in the Zhujiangkou Basin (Shao et al. 2007). Late Oligocene tectonic activities also caused diagenetic overprinting on fossil remnants. Below the slumped section at Site 1148, foraminiferal tests are re-crystallized and register strongly depleted oxygen isotope values, siliceous fossils have changed from opal-A toward the cristobalite dominated opal-CT, and fish teeth are brownish colored probably resulting from thermal alteration, all markedly different from those in the Miocene deposit overlying the slump (Wang P. et al. 2003). The late Oligocene unconformity is ubiquitous in many SCS shelf-slope basins, where it separates the Paleogene syn-rift, usually non-marine deposits from the Neogene post-rift marine deposits (Chapter 3) and represents a major tectonic event in East Asia.

Since 23 Ma, the SCS basin entered a stage of significant subsidence, with relatively low sedimentation rates of ~ 15 m/myr at Site 1148. Benthic foraminifera and ostracods from the site indicate a remarkable increase in water depth from an upper slope setting of $\sim 2,000$ m in the Oligocene to a lower slope setting at $\sim 3,000$ m in the early middle Miocene (Chapter 6) before spreading stopped at about 16 Ma, which was apparently responding to intensified Asia-Australia-Pacific collision. At the time, however, completely different depositional environments existed near-shore. In the Oligocene, near-shore sediments were characterized by thin-layered sandstones containing fresh-water phytoplankton (Wang P. et al. 2003). A reduction in terrigenous input coupled with increased topographic variations since the end of the Oligocene provided favorable conditions for reef development

and, by the early to middle Miocene, carbonate reefs achieved the broadest distribution (Chapter 4). Seafloor spreading ended at ~ 16 Ma when the southward migrating Nansha terrains collided with the SCS southern margin including Borneo (Hutchison 2004). Marking this event in the south was a prominent middle Miocene unconformity, together with widespread subduction and/or subsidence along the southern margin. At Site 1148 in the northern SCS, the 16 Ma event caused abrupt changes in elemental ratios and in grain size of terrigenous sediments (Li X. et al. 2003; Shao et al. 2004).

Post-Spreading Stage Since the Late Miocene

Before and during spreading, the SCS basin was surrounded by China-Indochina landmass to its north and west, and by Sundaland to its southwest (Hall and Morley 2004), leaving only the eastern and southeastern sides open to the Pacific Ocean. After spreading, however, the sea basin has been successively blocked by island arcs including Borneo, Palawan, Philippines and Taiwan on its southeastern and eastern sides along the western margin of the Philippine Sea plate. The closure of the SCS was associated with Asia-Australia collision in the south and with the rotation of the Philippine Sea plate in the east (Hall 2002).

Australia-Asia collision began in Sulawesi at about 25 Ma, leading to the anti-clockwise rotation of Borneo and perhaps also to the final stop of SCS spreading at 16 Ma and the subsequent final closure of the SCS in the south (Chapter 2). Comparison between benthic isotope curves from ODP Site 1148 and from other oceanic localities reveal lighter $\delta^{18}\text{O}$ values before 16 Ma and lighter $\delta^{13}\text{C}$ values after 16 Ma in the SCS records (Fig. 8.1). At ~ 16 Ma, benthic foraminifera changed from *Stilostomella* dominating to *Oridorsalis umbonatus* dominating, and carbonate dissolution also enhanced with a dissolution D2 event (Chapter 6). These changes in isotopes, benthic fauna and dissolution imply a different deep water in the post-spreading SCS, possibly caused by a change in the deep water source after the closure from the south.

The anticlockwise rotation of the Philippine Sea plate resulted in a stepwise closing of the SCS basin on the eastern side (Hall 2002) (Chapter 2). Collision of the Luzon Arc with the Asian Plate started ~ 6.5 Ma ago and subsequently contributed to the emergence of Taiwan and formation of the present Bashi Strait (Huang C. et al. 1997) (Fig. 2.26). The closure isolated the sea basin almost completely from the open ocean, leaving the Bashi (Luzon) Strait as the only connection passage with a sill depth of $\sim 2,400$ m. The Bashi Strait and its intermediate sill depth play a critical role in the establishment of the modern SCS oceanographic features: a basin-wise gyre, upwelling along the eastern and western coasts, its sensitivity to monsoon-induced seasonality, and a short residence time (50 yr or less) of its uniform deep water (Chapter 2). Nevertheless, the closure in the south and in the east has mainly involved a stepwise process. Benthic foraminiferal turnover data, for example, imply that the modern sill depth in the Bashi Strait was formed over the mid-Pleistocene period, around 0.9 Ma (Li Q. et al. 2008).

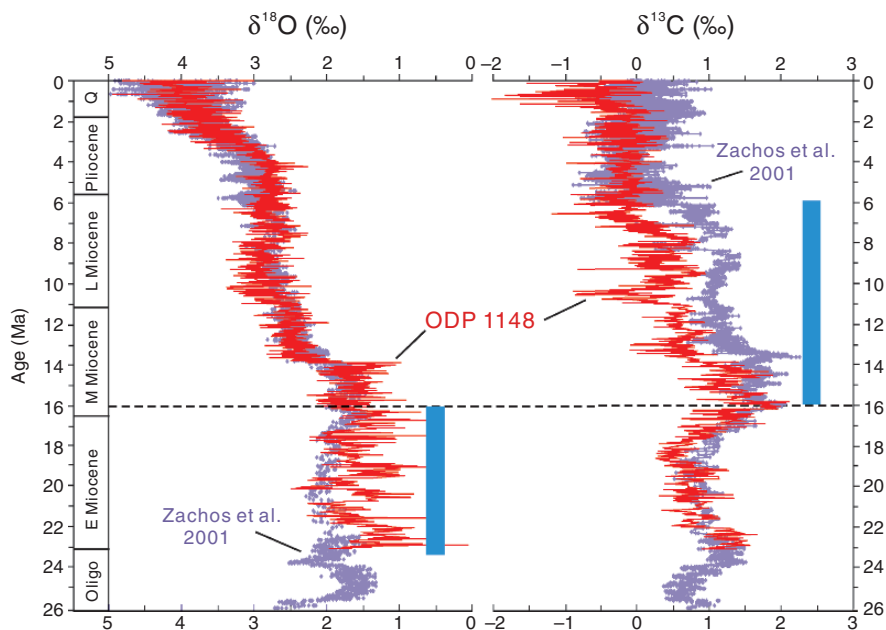


Fig. 8.1 Comparison of benthic foraminiferal oxygen and carbon isotopes between ODP Site 1148 and the global average from Zachos et al. (2001) reveals lighter SCS $\delta^{18}\text{O}$ before ~ 16 Ma and lighter SCS $\delta^{13}\text{C}$ after ~ 16 Ma (vertical blue bars), indicating an impact on the local record by different deep water regimes before and after the end of seafloor spreading at ~ 16 Ma

Another remarkable change in the post-spreading stage was the drastic increase of the sedimentation rates of terrigenous materials since the last 3 myr on the northern slope of the SCS (Fig. 8.2). This was related to continental uplift and to the formation of continental shelves and large deltas along the northern margin of the SCS (Wang P. et al. 2003).

8.2 Evolution of the East Asian Monsoon

Summer Monsoon and Chemical Weathering

Until recently, our knowledge of the monsoon history in East Asia relied largely on terrestrial records. Pollen and paleobotanical data from 120 on- and off-shore sites in China, together with lithological indicators, were used by Sun and Wang (2005) to reconstruct the distribution patterns of arid vs humid climates for five Cenozoic epochs. The results support an earlier notion that a broad arid zone was stretching across China in the Paleogene, but retreated to the northwest by the end of the Oligocene, indicating a transition from a planetary to monsoonal system in atmospheric circulation (Sun and Wang 2005). This is well in line with the discovery of the Miocene loess profile at Qin'an (Guo et al. 2002) and paleo-climate numerical modeling.

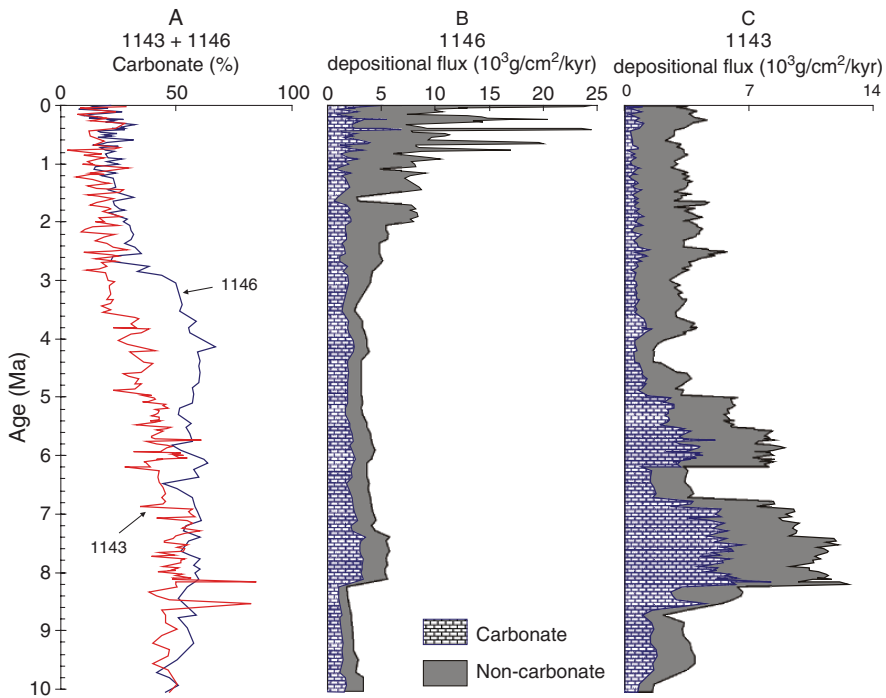
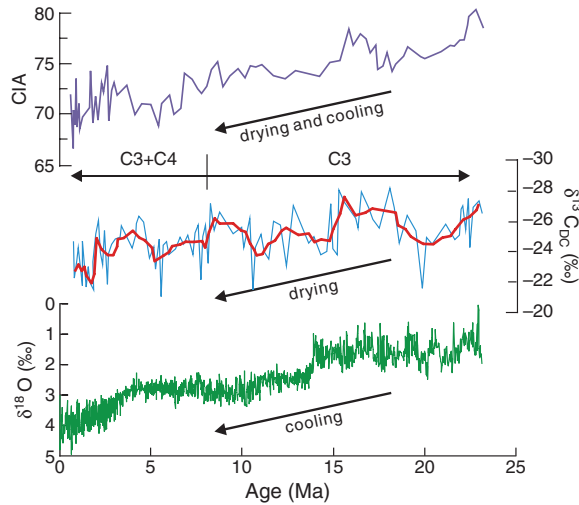


Fig. 8.2 Comparison between carbonate percentages at ODP Sites 1146 and 1143 (A) and mass accumulation rates of carbonate and non-carbonate at Site 1146 (B) and Site 1143 (C) indicates a shift of intensive depositional activities from the southwest (1143) at ~ 8 Ma to the northern South China Sea (Site 1146) in the last 2 myr

Today, deep-sea sediment sequences from the SCS open up a new approach for exploring the monsoon history. These long sequences provide two kinds of information essential to reconstructing monsoon variability: records of terrestrial processes such as precipitation and weathering, and records of marine processes such as upwelling and productivity. At ODP Site 1148 in the northern SCS, for example, a series of element ratios (Al/Ti, Al/K, Rb/Sr and La/L) increased abruptly around 29.5 Ma, in the early stage of the seafloor expanding of the SCS (Li X. et al. 2003). As the element ratios are indicative of the intensity of chemical weathering, their increases at ~ 29.5 Ma imply a period of enhanced humidity. Given the close tie between precipitation and summer monsoon in the region, further studies are needed to find out whether this was related to the inception of the East Asian Monsoon system.

The Neogene history of chemical weathering in South China was reconstructed on the basis of the chemical index of alteration (CIA) and elemental ratios (e.g., Ca/Ti, Na/Ti, Al/Ti, Al/Na, Al/K, and La/Sm) that are sensitive to chemical weathering from ODP Site 1148. The results indicate a warm and humid climate in South China during the early Miocene, but humidity decreased from the early Miocene to Present with several fluctuations centering respectively at about 15.7 Ma, 8.4 Ma,

Fig. 8.3 Secular variations of the CIA (chemical index of alteration) values, black carbon $\delta^{13}\text{C}$, and benthic foraminifer $\delta^{18}\text{O}$ at ODP Site 1148 indicate weakening of East Asian summer monsoon on a continuous drying background over the last 20 myr (from Wei et al. 2006)



and 2.5 Ma, coincident with global cooling since the middle Miocene (Fig. 8.3) (Wei et al. 2006). A similar trend found in black carbon $\delta^{13}\text{C}$ records from the same site indicates an increase of C_4 plants in vegetation over the Neogene, which implies seasonal precipitation and intensification of seasonal contrast in humidity (Fig. 8.3) (Jia et al. 2003). Therefore, the influence of East Asian summer monsoon in this region has decreased continuously since the early Miocene on a general drying background (Wei et al. 2006).

Winter Monsoon and North-South Contrast

Oceanographically, the modern SCS can be divided into two parts by the cross-basin eastward jet at approximately 10°N , 110°E to 18°N , 120°E (Fig. 2.8). The prevailing climate control is the East Asian Monsoon in the northern part, whereas the southern part belongs in the Western Pacific Warm Pool (WPWP). As the influence of the winter monsoon is much more significant than that of summer monsoon in the northern SCS, the north-south contrast in the SCS climate has been mainly due to the development and intensity of the winter monsoon, as demonstrated by Plio-Pleistocene records at ODP Site 1146 from the north and ODP Site 1143 from the south.

The subsurface planktonic foraminifer *Neogloboquadrina dutertrei* is a useful proxy for winter monsoon in the SCS (Chapter 5). At Site 1146, its increase in percentage at 7.6 Ma and further increases from 3.2 to 2.0 Ma indicate several stages of enhanced winter monsoon and increased productivity. In contrast, the *Neogloboquadrina* group displays an opposite abundance trend at Site 1143 with lower percentages from ~ 4 to ~ 2 Ma (Fig. 5.17) (Li B. et al. 2004). The divergence between the two sites was likely caused by the late Pliocene development of the winter monsoon on one hand and that of the WPWP on the other.

The deep-dwelling planktonic foraminifer *Pulleniatina obliqueloculata* is characteristic of low-nutrient, warm water in the SCS. In Pleistocene interglacial periods, the relative abundance of this species increased in the northern but declined in the southern SCS (Fig. 8.4). However, its decline over interglacials at Site 1143 in the south did not start until ~ 0.85 Ma, during the mid-Pleistocene revolution (MPR), while its records before this time show no difference between the two sites (Fig. 8.4) (Xu et al. 2005). A similar post-MPR reversal also occurred in opal% records at Site 1143 (Wang R. et al. 2007), indicating a change in productivity (Fig. 8.4). Together, these observations imply that (1) a more saline subsurface water in the southern SCS during glacials after the MPR was probably caused by stronger stratification in the upper water column due to high precipitation, and (2) the East Asian winter monsoon has drastically increased its influence on the northern SCS climate after the MPR due to the enlarged boreal ice sheet. Therefore, coupled regional and global factors have driven further enhancement of the N-S contrast in the SCS region.

East and South Asian Monsoons

The afore-mentioned new findings are at odds with the previous notion that the East Asian Monsoon basically follows the path of the Indian Monsoon and has been strengthening since ~ 8 Ma and ~ 3 Ma. Indeed, climate seasonality in East Asia has been strengthened throughout the Neogene, but this is basically on account of the winter monsoon, not the summer monsoon. Marine productivity in the Indian Ocean is driven by the summer monsoon, but in the northern SCS it is mainly driven by the winter monsoon. For example, although an increase in the abundance of *N. dutertrei* group at 7.6 Ma represents a region-wide event in the SCS, its increases from 3.2 to 2.0 Ma appear to have begun first in the north, at Site 1146 (Fig. 5.27), indicating winter monsoon enhancement. These SCS records, therefore, demonstrate similar stages in the development of the East and South Asian monsoons during the late Neogene, with an enhanced winter monsoon over East Asia being the major difference (Wang P. et al. 2005).

As monsoon variability depends on seasonal and spatial distribution of insolation, orbital cyclicity is inherent in both winter and summer monsoon variations. While the winter monsoon in Asia responds to the development of boreal ice-sheet, the summer monsoon is closely associated with low-latitude processes and particularly sensitive to precession forcing and to eccentricity cycles which modulate the amplitude of climate precession (Ruddiman 2001). For example, fluctuations in the K/Si ratio from 3.2 Ma to 2.5 Ma at ODP Site 1145, northern SCS, show clearly

Fig. 8.4 North-South contrasts are recorded in the abundance variations of *P. obliqueloculata* and opal in their response to glacial cycles at northern Sites 1146 and 1144 and at southern Site 1143: (A) planktonic $\delta^{18}\text{O}$ at Site 1146, (B) *P. obliqueloculata*% at Site 1146, (C) benthic $\delta^{18}\text{O}$ at Site 1143, (D) *P. obliqueloculata*% at Site 1143, (E) planktonic $\delta^{18}\text{O}$ at Site 1144, (F) opal% at Site 1144, and (G.) opal% at Site 1143. *P. obliqueloculata*% data were from Xu et al. (2005), and opal% data from Wang R. et al. (2007)

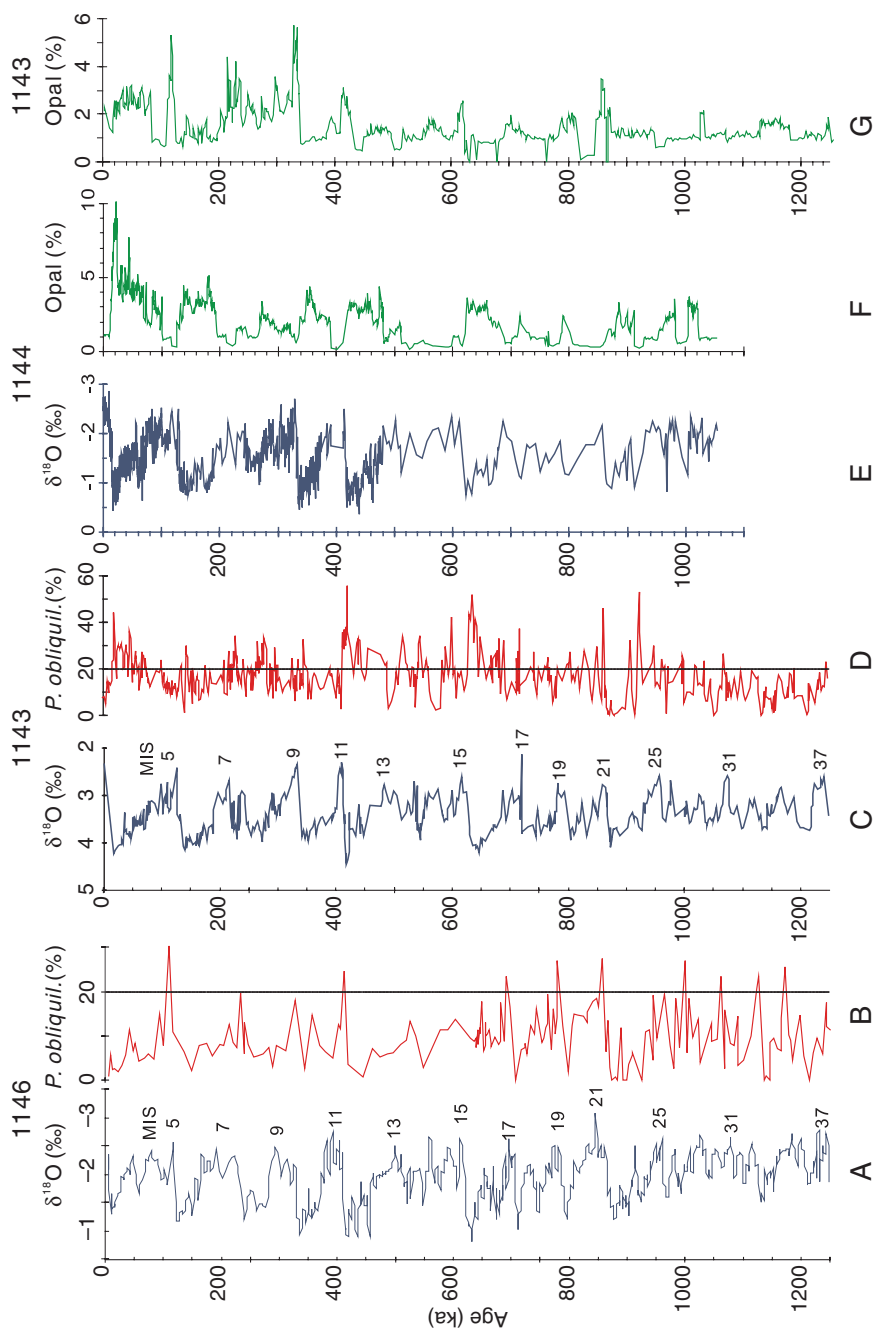


Fig. 8.4 (continued)

20 kyr precession and 400 kyr eccentricity cycles (Fig. 5.41) (Wehausen and Brumsack 2002). The 400 kyr long eccentricity cycle is best expressed in pre-Quaternary $\delta^{13}\text{C}$ records, such as at ODP 1143 (Wang P. et al. 2004). This long-eccentricity cyclicity in the oceanic carbon reservoir is believed to have originated from low-latitude chemical weathering, which in turn is affected by the summer monsoon (Chapter 7).

8.3 Evolution of Continent-Ocean Interactions

A series of marginal seas separates the largest Asia continent from the largest Pacific Ocean. All four major western Pacific marginal seas, the Sea of Okhotsk, the Sea of Japan, the East and South China Seas, are aligned in a NE-SW direction and connected to island arcs to the southeast. The marginal seas make up a distinct feature of the modern western Pacific and exert great influences on Asia-Pacific interactions (Wang P. et al. 2004).

Unlike the Sea of Japan or Sea of Okhotsk, the SCS produces neither deep nor intermediate water because of its low-latitude position and warm climate. Accordingly, deep water conditions in the SCS are favorable for preservation of carbonate and fossils which archive signals of Pacific influence. Ample sediment supply from a number of large rivers carries terrestrial information, and the resultant hemipelagic deposits are beneficial for high-resolution climate studies (Wang P. 1999). Meanwhile the basin-wide circulation gyre separates the central SCS from the river-dominated marginal parts, maintaining an oligotrophic, open-water condition in the basin. Therefore, the SCS is not only the largest marginal sea in the western Pacific but also the best witness and history narrator of Asia-Pacific interactions. Because its sediment sequence is better preserved than those of most western Pacific localities, the SCS has a critical role to play in providing paleoceanographic records of the West Pacific for many years to come.

The opening of the SCS, the Japan Sea and probably the Okhotsk Sea all dated back to the late Oligocene-middle Miocene (30–15 Ma), broadly corresponding to the onset of a period of major deformation in Tibet. A causal relationship has been proposed between the opening of marginal basins and India-Asia collision. Other theories include subduction-driven extensional forces due to collision between Eurasian and Pacific plates. However, the mechanism responsible for the opening of the marginal seas remains unclear partly because the role of Pacific oceanic tectonics is not well constrained. Nevertheless, the formation of the marginal basins has changed the trajectory of material flux and energy flow between the Asian continent and the Pacific Ocean. Even the formation of the WPWP and the Kuroshio Current depends on the presence of the island arcs as well as their associated marginal seas (Wang P. 2004). In the Paleogene, the area of the present SCS lied in the junction between the Tethys and Pacific oceans. A clearer picture of the Paleogene West Pacific without marginal seas is expected from in-depth studies of the Proto-SCS and the narrow gulf that subsequently evolved into the present northern SCS.

The hemipelagic deposits of the SCS contain rich information on the environmental evolution of the East Asian continent, ranging from reorganization of drainage systems (Chapter 4) to succession of vegetation covers (Chapter 5). The Red River, for example, has a small modern drainage area and exerts a very limited influence on the modern SCS oceanography, but the huge deltaic sediment package to over 14 km thick lying offshore the river mouth in the Yinggehai Basin (Chapter 3) demands the role of a more dynamic Paleo-Red River in the Cenozoic. The accelerated deposition rate of non-carbonate sediments off the modern Pearl River delta since 3 Ma (Fig. 8.2) indicates greater fluvial supply and enhanced transport of shelf deposits to the slope in responding to glacial cycles. Similarly, large amplitude changes in pollen assemblages in glacial cycles since MIS 6 suggest that the extensive northern SCS shelf formed only ca. 150 ka ago (Sun et al. 2003), which exemplifies the most recent development in sea-land interactions in the SCS.

References

- Guo Z.T., Ruddiman W.F., Hao Q.Z., Wu H.B., Qiao Y.S., Zhu R.X., Peng S.Z., Wei J.J., Yuan B.Y. and Liu T.S. 2002. Onset of Asian desertification by 22 Myr ago inferred from loess deposits in China. *Nature* 416: 159–163.
- Hall R. 2002. Cenozoic geological and plate tectonic evolution of SE Asia and the SW Pacific: computer-based reconstructions, model and animations. *J. Asian Earth Sci.* 20: 353–431.
- Hall R. and Morley C.K. 2004. Sundaland basins. In: Clift P., Wang P., Kuhnt W. and Hayes D. (eds.), *Continent-Ocean Interactions within East Asian Marginal Seas*. AGU Geophys. Monogr. 149: 55–85.
- Hsu S.K., Yeh Y.C., Doo W.B. and Tsai C.H. 2004. New bathymetry and magnetic lineations identifications in the northernmost South China Sea and their tectonic implications. *Mar. Geophys. Res.* 25: 29–44.
- Huang C.Y., Wu W.Y., Chang C.P., Tsao S., Yuan P.B., Lin C.W. and Xia K.Y. 1997. Tectonic evolution of accretionary prism in the arc-continent collision terrane of Taiwan. *Tectonophysics* 281: 31–51.
- Huang L. 1997. Calcareous nannofossil biostratigraphy in the Pearl River Mouth basin, South China Sea, and Neogene reticulofenestra coccolith size distribution pattern. *Mar. Micropaleontol.* 32: 3–29.
- Hutchison C.S. 2004. Marginal basin evolution: the southern South China Sea. *Mar. Petroleum Geol.* 21: 1129–1148.
- Jia G., Peng P., Zhao Q. and Jian Z. 2003. Changes in terrestrial ecosystem since 30 Ma in East Asia: Stable isotope evidence from black carbon in the South China Sea. *Geology* 31: 1093–1096.
- Li B., Wang J., Huang B., Li Q., Jian Z. and Wang P. 2004. South China Sea surface water evolution over the last 12 Ma: A south-north comparison from ODP Sites 1143 and 1146. *Paleoceanography* 19: PA1009, doi:10.1029/2003PA000906.
- Li Q., Wang P., Zhao Q., Shao L., Zhong G., Tian J., Cheng X., Jian Z. and Su X. 2006. A 33 Ma lithostratigraphic record of tectonic and paleoceanographic evolution of the South China Sea. *Mar. Geol.* 230: 217–235.
- Li Q., Wang P., Zhao Q., Tian J., Cheng X., Jian Z. Zhong G. and Chen M. 2008. Paleoceanography of the mid-Pleistocene South China Sea. *Quat. Sci. Rev.* 27: 1217–1233.
- Li X., Wei G., Shao L., Liu Y., Liang X., Jian Z., Sun M. and Wang P. 2003. Geochemical and Nd isotopic variations in sediments of the South China Sea: a response to Cenozoic tectonism in SE Asia. *Earth Planet. Sci. Lett.* 211: 207–220.
- Ruddiman W.F. 2001. *Earth's Climate. Past and Future*. W.H. Freeman and Company, N.Y., 465pp.

- Shao L., Li X., Geng J., Pang X., Lei Y., Qiao P., Wang L. and Wang H. 2007. Deep water bottom current deposition in the northern South China Sea. *Sci. China (D)* 50(7): 1060–1066.
- Shao L., Li X., Wang P., Jian Z., Wei G., Pang X. and Liu Y. 2004. Sedimentary record of the tectonic evolution of the South China Sea since the Oligocene. *Advances Earth Sci.* 19: 539–544 (in Chinese).
- Sun X. and Wang P. 2005. How old is the Asian monsoon system? – Palaeobotanical records from China. *Palaeogeogr., Palaeoclimatol., Palaeoecol.* 222: 181–222.
- Sun X., Luo Y., Huang F., Tian J. and Wang P. 2003. Deep-sea pollen from the South China Sea: Pleistocene indicators of East Asian monsoon. *Mar. Geol.* 201: 97–118.
- Wang P. 1999. Response of Western Pacific marginal seas to glacial cycles: Paleooceanographic and sedimentological features. *Mar. Geol.* 156: 5–39.
- Wang P. 2004. Cenozoic deformation and the history of sea-land interactions in Asia. In: Clift P., Wang P., Kuhnt W. and Hayes D. (eds.), *Continent-Ocean Interactions in the East Asian Marginal Seas*. AGU Geophys. Monogr. 149: 1–22.
- Wang P., Clemens S., Beaufort L., Braconnot P., Ganssen G., Jian Z., Kershaw P. and Sarnthein M. 2005. Evolution and variability of the Asian monsoon system: state of the art and outstanding issues. *Quat. Sci. Rev.* 24: 595–629.
- Wang P., Tian J., Cheng X., Liu C. and Xu J. 2004. Major Pleistocene stages in a carbon perspective: The South China Sea record and its global comparison. *Paleoceanography* 19: doi: 10.1029/2003PA000991.
- Wang P., Zhao Q., Jian Z., Cheng X., Huang W., Tian J., Wang J., Li Q., Li B. and Su X. 2003. Thirty million year deep-sea records in the South China Sea. *Chinese Sci. Bull.* 48(23): 2524–2535.
- Wang R., Jian Z., Xiao W., Tian J., Li J., Chen R., Zheng L. and Chen J. 2007. Quaternary biogenic opal records in the South China Sea: linkages to East Asian monsoon, global ice volume and orbital forcing. *Sci. China (D)* 50(5): 710–724.
- Wehausen R. and Brumsack H.J. 2002. Astronomical forcing of the East Asian monsoon mirrored by the composition of Pliocene South China Sea sediments. *Earth Planet. Sci. Lett.* 201: 621–636.
- Wei G.J., Li X., Liu Y., Shao L. and Liang X. 2006. Geochemical record of chemical weathering and monsoon climate change since the early Miocene in the South China Sea. *Paleoceanography* 21: PA4214, doi: 10.1029/2006PA001300.
- Xu J., Wang P., Huang B., Li Q. and Jian Z. 2005. Response of planktonic foraminifera to glacial cycles: Mid-Pleistocene change in the southern South China Sea. *Mar. Micropaleontol.* 54: 89–105.
- Zachos J., Pagani M., Sloan L., Thomas E. and Billups K. 2001. Trends, rhythms, and aberrations in global climate 65 Ma to present. *Science* 292: 686–693.